ECCOMAS Congress 2016
VII European Congress on Computational Methods in Applied Sciences and Engineering
M. Papadrakakis, V. Papadopoulos, G. Stefanou, V. Plevris (eds.)
Crete Island, Greece, 5–10 June 2016

DYNAMICAL ANALYSIS OF PLATE MODELS WITH UNCERTAIN STRUCTURAL PROPERTIES USING THE INTERVAL FIELD METHOD

Maurice Imholz[1], **Dirk Vandepitte**[1], **and David Moens**[1]

[1]KU Leuven, Department. of Mechanical Engineering
Celestijnenlaan 300B, 3001 Heverlee, Belgium
e-mail: maurice.imholz@kuleuven.be - dirk.vandepitte@kuleuven.be - david.moens@kuleuven.be

Keywords: possiblistic analysis, interval analysis, interval fields, Finite Element analysis

Abstract. *In uncertainty quantification, interval arithmetic provides an appropriate procedure when little knowledge is available on the nature of the probability distribution of uncertain or imprecise quantities. This commonly occurs in engineering applications due to subjective knowledge or incomplete availability of test data. Intervals are by definition unable to take into account dependent input and output quantities, which forces the assumption of independency when applying them. This is a severe limitation on the accuracy of the analysis as dependency is always present to some extent. The concept of interval fields (IF) [1] provides a solution by defining non-deterministic fields using interval parameters. In its simplest form [2], the field is expressed as a weighted sum of basis functions, the weights being modelled using interval parameters. The dependency within the field is then captured by the basis functions, which describe the spatial nature of dependency, whereas the magnitude of uncertainty is captured by the weights. Field parameters are usually associated to geometric quantities (such as plate thickness), but they can be applied generally whenever multiple uncertain input or output quantities are involved. Both at the input and output side of a numerical analysis, IF can be used for a more realistic description of the estimated uncertainty. At the input side, taking into account dependency reduces overestimation on the output uncertainty bounds. At the output side, it is important that a realistic uncertain set of output quantities is represented as closely as possible without adding conservatism, as this corrupts the results of possible postprocessing or follow-up analysis. The application of IF here provides an important step towards achieving this goal.*

This paper aims to apply IF to analyse structural Finite Element models with uncertain structural properties. The property of interest in this paper will be the E-modulus. The concept of IF will be used to model spatial dependency within this parameter and will lead to a more accurate estimation of the output uncertainty.

1 INTRODUCTION

1.1 Possibilistic uncertainty analysis

In numerical modelling, Uncertainty Analysis (UA) concerns the identification and quantification of possible sources of uncertainty within a model, with the purpose of obtaining information on the uncertainty present in the model's relevant output. In this context, a non-deterministic approach of the modelling process is essential. Instead of the classical deterministic representation of model parameters, non-deterministic concepts are used to open up the possiblity of representing uncertainty on the parameters. These concepts can be divided in two groups. Firstly, *probabilistic analysis* uses probability distributions and stochastic parameters to assign a finite probability to a parameter having a certain value. Secondly, *possiblistic analysis* omits the concept of probability and only concerns the possiblity of a parameter having a certain value. Intervals, fuzzy numbers and convex regions are commonly used for this purpose. The choice of which approach to follow is usually based on the availability of knowledge on the uncertainty that is present. The definition of probability functions requires extensive knowledge on the uncertain parameter of interest. In practise, the Gaussian distribution is often assumed to estimate the stochastic moments, but the infinite base of this distribution poses a fundamental objection to this. Also, to accurately estimate stochastic parameters, a lot of experimental data is required. When experimental data is hard or expensive to obtain or their quality is questionnable, possibilistic analysis becomes an interesting alterative. The interval approach provides a much lower threshold to perform a non-determistic analysis than the stochastic approach. Also numerically, experiments can be expensive in terms of computational time, limiting the use of sample based stochastic techniques such as Monte Carlo Sampling. This paper will focus on the interval approach as basic tool for possibilistic analysis, and apply it in the context of a structural Finite Element (FE) model.

1.2 Modelling geometric uncertainty

Uncertain parameters in FE models typically have a spatial character: material properties such as density and Young's modulus or geometric properties such as plate thicknesses are geometrically oriented in space. In uncertain context, these parameters can show variability over the spatial domain, referred to as *geometric variability*. In FE-models, such a geometric parameter is discretised to the elements, leading to a set of discrete variables representing that variable in each element of the model. According to the possibility of geometric variability, the value in each element can vary separately, leading to different values in each element. However, some degree of dependency will usually be present and the value in different elements can not vary independently. Here the interval concept poses a problem. The uncertainty in each element could be captured by an interval parameter marking the bounds of the variation, but interval parameters are by definition incapable of incorporating the dependency present in the spatial domain. To mark the uncertainty present in such *field parameters* using a possiblistic technique, the *interval field* technique can be used as illustrated in equation 1. In its simplest form, an interval field consists of basis functions $\phi(\mathbf{r})$ representing the dependency and interval coefficients α^I representing the uncertainty.

$$y^I(\mathbf{r}) = \sum_{i=1}^{n} \alpha^I \phi_i(\mathbf{r}) \tag{1}$$

1.3 Dependency in a possibilistic context

For non-deterministic field parameters, a parameter needs to be defined that represents the level of dependency within the field. In stochastic FE context, as dictated by the theory of random fields (RF) [3], the correlation length is often used as measure for the dependency in the spatial domain. In this case, the correlation between values in different points is made a function of the distance between the points, with the correlation length $L_\rho$as governing parameter. The example of an exponential relationship is given in equation 2.

$$COV(x(\mathbf{r}_1), x(\mathbf{r}_2)) = \exp\left(\frac{\|\mathbf{r}_1 - \mathbf{r}_2\|}{L_\rho}\right) \tag{2}$$

As correlation is only defined in stochastic context, use of this parameter in possibilistic context is not straightforward. The authors proposed the use of the *maximum gradient* as parameter governing the dependency in the field, as this better fits the possiblistic approach than the correlation. The subject of this paper will be to apply this approach to identify the variability of the natural frequencies of a steel plate with geometrically varying Young's modulus.

2 MODELLING THE INPUT UNCERTAINTY: THE LOCAL INTERVAL FIELD DECOMPOSITION

2.1 General concept

Referring to [4], the Local Interval Field Decomposition (LIFD) was introduced to incorporate the maximum derivative constraint in a 1D non-deterministic field. This decomposition method puts a radial-based basis function and corresponding interval parameter in each element of the FE model. Therefore, *the dimensionality of the uncertainty is equal to the number of elements*. The reason for this approach is that, regardless of the level of dependency, each element can (at least partially) determine its own value and as a result, the dimensionality is equal to the number of elements. However, the issue of the dependency between the elements still stands. Through the LIFD, the initial interdependent interval set is transformed to an interval set of (at least) equal size that is *independent*, while still obeying the maximum derivative constraint. The following section considers the expansion of the LIFD to 2D non-deterministic fields.

2.2 Derivation of the LIFD in 2 dimensions

Suppose we have a field parameter $u(x, y)$ with x, y the spatial coordinates in a 2D-plane. We define the gradient $\nabla u(x, y)$ and its norm G as:

$$\nabla u(x, y) = \left(\frac{\partial u(x, y)}{\partial x}, \frac{\partial u(x, y)}{\partial y}\right) \tag{3}$$

$$G = \sqrt{\left(\frac{\partial u(x, y)}{\partial x}\right)^2 + \left(\frac{\partial u(x, y)}{\partial y}\right)^2} \tag{4}$$

For a certain realisation $\tilde{u}(x, y)$, the maximal and minimal value for that specific realisation are defined as $\max_{x,y} \tilde{u}(x, y) = \overline{u}$ and $\min_{x,y} \tilde{u}(x, y) = \underline{u}$. The LIFD in 2D will write the non-determistic field $u(x, y)$ as an interval field $u^I(x, y)$ in the form of equation 1 that obeys the following statements:

1. $\forall(\tilde{x}, \tilde{y}) \in \Omega : U_{min} \leq u(\tilde{x}, \tilde{y}) \leq U_{max}$

2. $\forall (x,y) \in \Omega : \sqrt{\left(\frac{\partial u(x,y)}{\partial x}\right)^2 + \left(\frac{\partial u(x,y)}{\partial y}\right)^2} \leq G_{max}$

3. $\forall \tilde{u}(x,y) : \overline{u} - \underline{u} \leq D_{max}$

The parameters G_{max}, U_{min}, U_{max} and D_{max} can be independently set. The first statement demands that the absolute bounds on the field parameter U_{min} and U_{max} are never exceeded. The second statement demands that the norm of the gradient never exceeds a preset value. This statement accounts for the dependency in the field. The third statement puts a bound on the difference between the maximal and minimal value of any realisation of the interval field. The objective of the LIFD is to obey the statements using the four governing uncertainty parameters mentioned above with an explicit interval field description with *independent* interval coefficients.

The only freedom we have is the shape of the basis functions. In the 2D-case, the basis functions have the following properties:

1. All ϕ_i are identically shaped radial basis functions.

2. A single ϕ_i is positioned at each element at location $\mathbf{r}_i$ of the FE mesh.

3. All ϕ_i are piecewise second order polynomial functions so the first derivatives are continuous.

figure 1 illustrates the shape of a basis function. For a basis function centered at element i with coordinates x_i and y_i, the mathematical definition is given by equation 5.

$$\phi_i(x,y) = \begin{cases} 0 & R < \sqrt{(x-x_i)^2 + (y-y_i)^2} \\ \frac{2(r-r_i+R)^2}{R^2} & \frac{R}{2} < \sqrt{(x-x_i)^2 + (y-y_i)^2} \leq R \\ 1 - \frac{2(r-r_i)^2}{R^2} & 0 \leq \sqrt{(x-x_i)^2 + (y-y_i)^2} \leq \frac{R}{2} \end{cases} \tag{5}$$

with $r = \sqrt{x^2+y^2}$ and $r_i = \sqrt{x_i^2 + y_i^2}$. To comply with all demands, the following explicit field is proposed:

$$u^I(x,y) = C^I + \sum_{i=1}^{n} a \cdot 1_i^I \cdot \phi_i(x,y,R), \tag{6}$$

with $C^I = \left\langle \underline{C} | \overline{C} \right\rangle$ and $1_i^I = \langle 0|1 \rangle$ defined as the *unity* interval. The four controllable parameters are $\underline{C}$, $\overline{C}$, a and R. A unique mapping between these parameters and the four global uncertainty pararmeters is given by equation 7:

$$\begin{aligned} U_{max} &= \frac{7\pi \cdot a \cdot R^2}{24 \cdot dx \cdot dy} + \overline{C} \\ U_{min} &= \underline{C} \\ G_{max} &= \frac{a \cdot R}{dx \cdot dy} \\ D_{max} &= \frac{7\pi \cdot a \cdot R^2}{24 \cdot dx \cdot dy} \end{aligned} \tag{7}$$

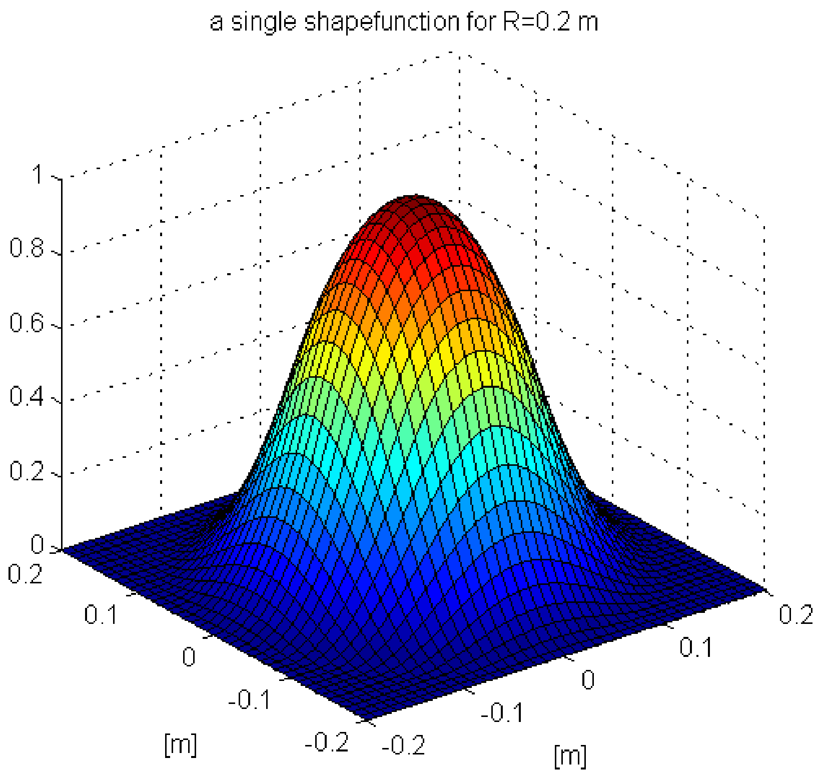

Figure 1: shape of a 2D radial basis function. Beyond a radius R from the center point, the basis function equals zero.

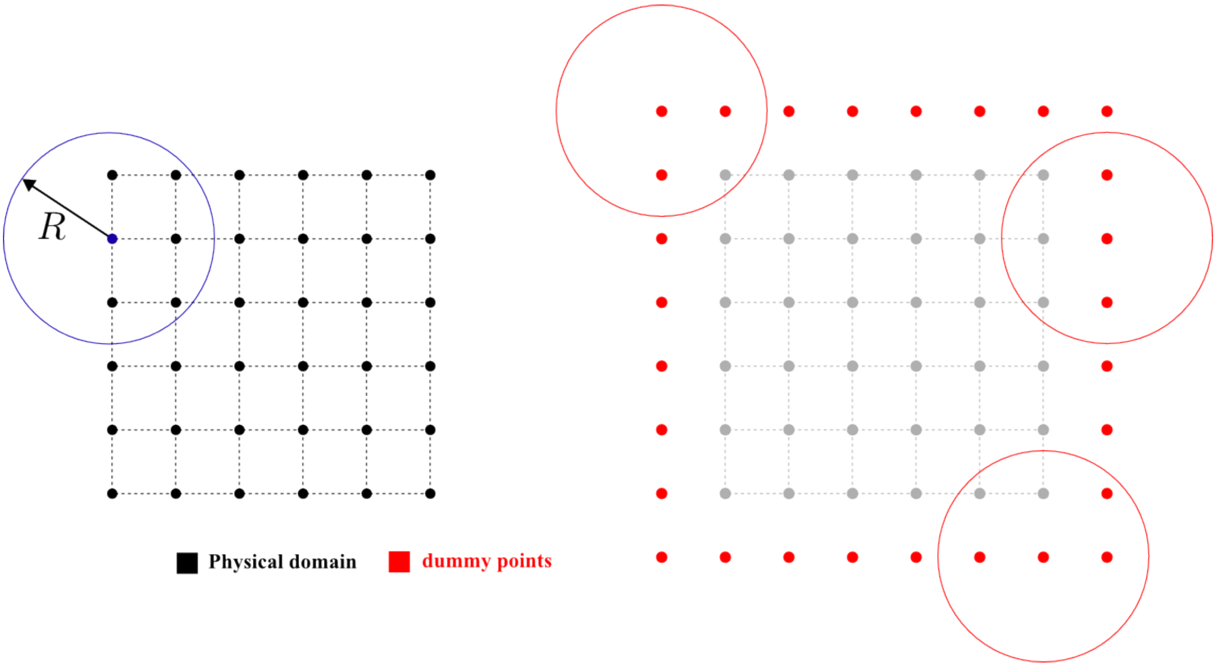

Figure 2: Illustration how dummy points are added beyond the physical domain to keep the maximum gradient constraint valid close to the edges.

With these relations, the four global uncertainty parameters can be independently set, leading to a unique field definition as in equation 6.

To ensure the maximum gradient constraint is kept over the entire domain, an adjustment is needed close to the edge of the domain. For points that lie within a distance R from a domain edge, the maximum constraint does not hold, because fewer basis functions have an effect in these points, leading to a smaller interval on the gradient in these points. To counter this, *dummy points* are added **beyond** the physical domain up to a distance R. The basis functions placed in these points lie partly in the physical domain and will ensure that the maximum gradient constraint is kept over the entire physical domain. Figure 2 shows the dummy points beyond the physical domain.

Figure 3 shows some realisations of a field within a rectangular plane for different values of R and a. One can clearly see how the combined choice of a and R produce more or less spatially dependent realisations.

3 PROPAGATING THE UNCERTAINTY: THE CONTINUOUS FIELD RESPONSE SURFACE

The analysis case in this paper will be the natural frequencies of a simple plate model with uncertain Young's modulus. The plate has a total of $20 \times 20 = 400$ elements, which leads to (at least) 400 interval parameters in the input field. To propagate this uncertain field to the output, a response surface will be defined. Assume we define a second order polynomial model on an output w within an input space $u_1, u_2, ..., u_n$ given by equation 8.

$$w = w_0 + \sum_{i=1}^{n} a_i u_i + \sum_{i=1}^{n} \sum_{j=1}^{n} b_{ij} u_i u_j \tag{8}$$

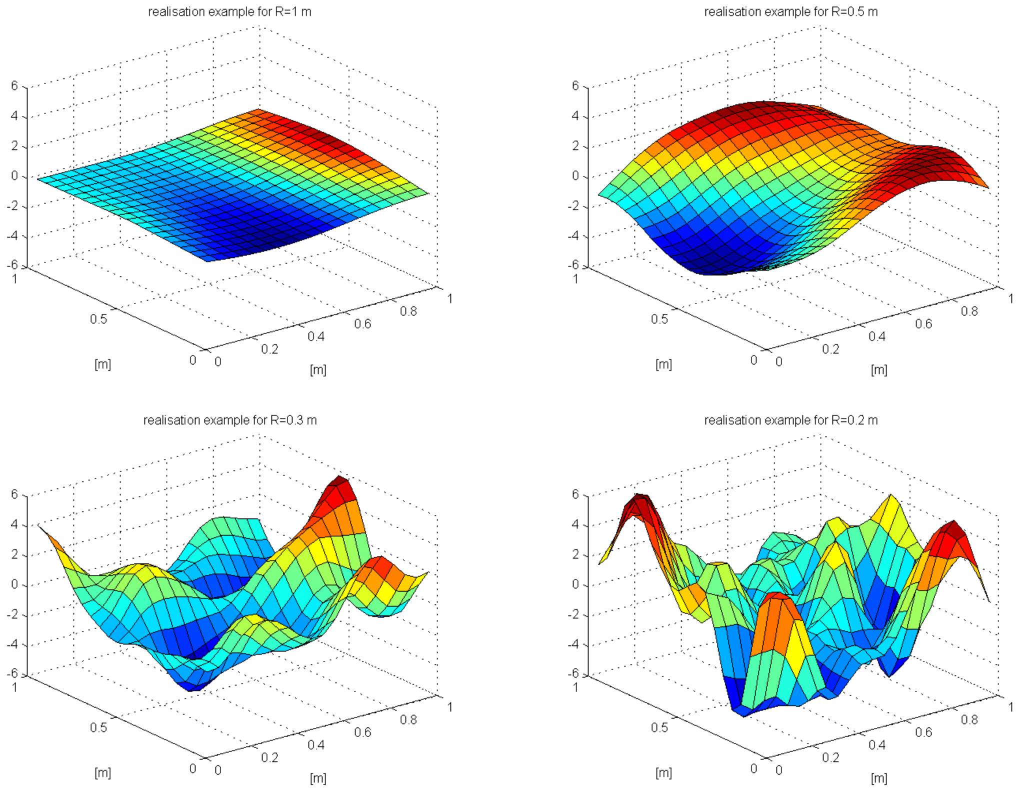

Figure 3: realisation examples for different values of R.

We assume n is a very large number, but all input parameters are instances of the same geometric parameter at different locations, e.g. the Young's modulus in each element of the FE-model. Obviously, determining the coefficients of such a high-dimensional model would require a very large amount of training samples, especially when the interaction terms are considered. To reduce the actual dimension of the response surface, we will take into account the high similarity of the input parameters. For example, the coefficients corresponding to the parameter value in adjacent elements have to be quite similar. The fact that the *coefficients are correlated in space* leads to a response surface description in terms of the spatial coordinates x and y, which the authors introduced earlier in [5], and is given by equation 9.

$$w = C + \iint_{x,y} a(x,y)u(x,y)dxdy + \iint_{x,y} b(x,y)u^2(x,y)dxdy + \iint_{x,y,\Delta x,\Delta y} q(x,y,\Delta x,\Delta y)u(x,y)u(x+\Delta x, y+\Delta y)dxdyd\Delta xd\Delta y \tag{9}$$

The discrete coefficients of the discrete model have been replaced by continuous *coefficient fields* that are defined over the spatial domain. The function also includes an interaction term which includes the product of the geometric parameter $u(x,y)$ at different elements in the model. Based on the first order approximation:

$$u(x_i+\Delta x, y_i+\Delta y) = u(x_i,y_i) + \Delta x\frac{\partial u(x,y)}{\partial x} + \Delta y\frac{\partial u(x,y)}{\partial y}, \tag{10}$$

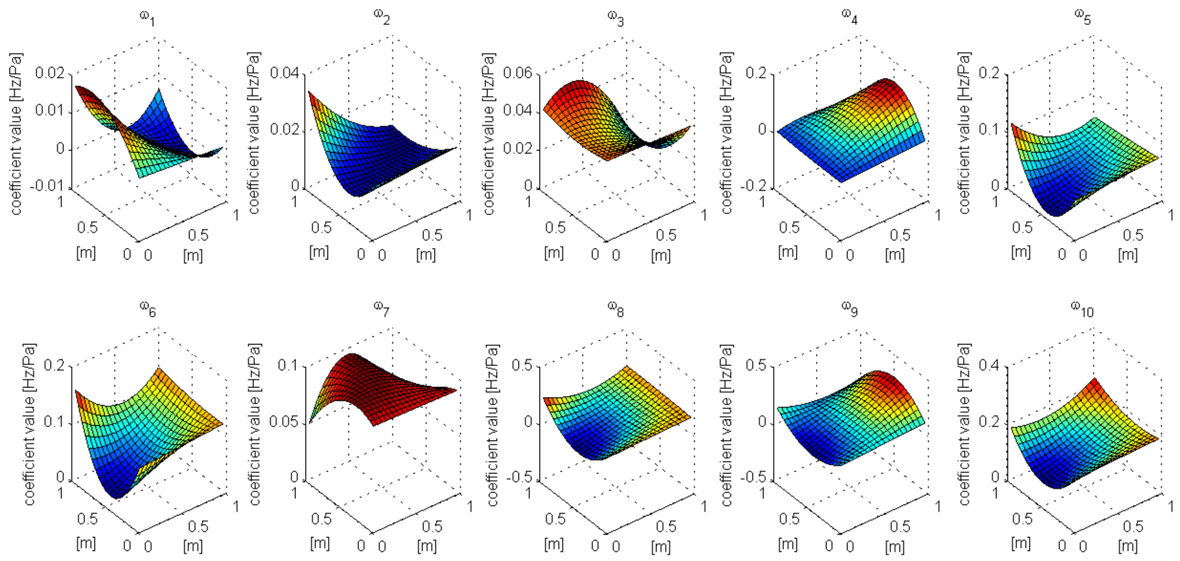

Figure 4: coefficient fields corresponding to each of the first 10 natural frequencies.

we replace this term by 2 terms including the product of the geometric parameter and its derivatives, leading to equation 11.

$$y = C + \iint_{x,y} a(x,y)u(x,y)dxdy + \iint_{x,y} b(x,y)u^2(x,y)dxdy +$$
$$\iint_{x,y} q_x(x,y)u(x,y)\frac{\partial u(x,y)}{\partial x}dxdy) + \iint_{x,y} q_y(x,y)u(x,y)\frac{\partial u(x,y)}{\partial y}dxdy) \tag{11}$$

For the training process, we assume that the *coefficient fields* $a(x,y)$, $b(x,y)$ etc. are continuous functions in the spatial domain, thereby transforming the training process to a much lower actual dimension. For example, a coefficient field a(x,y) with 400 discrete locations can be written with a 2D polynomial as in equation 12.

$$a(x,y) = a_{00} + a_{10}x + a_{01}y + a_{11}xy + a_{20}x^2 + a_{02}y^2 \tag{12}$$

This representation only has 6 unknown coefficients, so instead of determining all 400 coefficients independently, redefining the problem reduces this number to only 6.

4 APPLICATION: STEEL PLATE WITH UNCERTAIN STIFFNESS PROPERTIES

4.1 Coefficient functions

We now continue towards applying this continuous model on our analysis case. The coefficient fields $a(x,y)$, $b(x,y)$, etc. are determined by using a linear least-squares based algorithm. For the specific case of the plate frequencies, first order polynomials lead to errors of only 1%. The coefficient function for each of the 10 first eigenfrequencies are given in figure 4.

4.2 Resulting output field

With the response surface defined, we can very easily make the step towards an output interval field description. The interval field can be written as

$$u^I(x,y) = u_0(x,y) + \sum_{i=1}^{N_{ext}} \cdot 1_i^I \cdot \phi_i(x,y) \tag{13}$$

with N_{ext} the total number of elements and dummy points (figure 2). If we put this in equation 9, we obtain the following description of the output field:

$$\boldsymbol{\omega}^I = \boldsymbol{\omega}_0 + \sum_{i=1}^{N_{ext}} a \cdot \boldsymbol{\xi}^{(i)} \cdot 1_i^I \tag{14}$$

with $\boldsymbol{\omega}^I$ an interval vector with the 10 first natural frequencies in it. $\boldsymbol{\xi}^{(i)}$ are vectors with elements:

$$\boldsymbol{\xi}_j^{(i)} = \iint_{x,y} a_i(x,y)\phi_j(x,y)dxdy \tag{15}$$

4.3 Identifying the uncertain region

The resulting interval field has a total of N_{ext} terms. For ease of calculation, the interval parameters are depicted by normalized intervals $1_i^I = \langle 0|1 \rangle$.

The interval field mentioned above corresponds to an uncertain region of frequency combinations. Because the example considers only the first 10 natural frequencies, this is a 10-dimensional region. If we look at 2D projections of this region on all possible (ω_i, ω_j)-subspaces, we observe 'shuttle'-shaped regions, an example of which is given in figure 5. This is due to the monotonous behaviour of natural frequency w.r.t increasing stiffness. Such a shuttle shape has two cornerpoints corresponding to the input points where al inputs are at their lowest or highest value respectively. Between these points, two curves bound the uncertain region, an *upper* and a *lower* curve.

From the fields $\boldsymbol{\xi}^{(i)}$ we can reconstruct the 2D projections of the uncertain region. For frequencies ω_p and ω_q, we define the vector $\boldsymbol{\rho}^{(pq)}$ with elements $\rho_i^{(pq)} = \frac{\xi_i^{(p)}}{\xi_i^{(q)}}$. Define $\overset{+}{\boldsymbol{\rho}}^{(pq)}$ as the vector with the elements of $\boldsymbol{\rho}^{(pq)}$ sorted in ascending order, and $\overset{-}{\boldsymbol{\rho}}^{(pq)}$ as the vector with the elements of $\boldsymbol{\rho}^{(pq)}$ sorted in descending order. Additionally, we rearrange $\boldsymbol{\xi}^{(p)}$ and $\boldsymbol{\xi}^{(q)}$ so that (equation 16)

$$\overset{+}{\rho}_i^{(pq)} = \frac{\overset{+}{\xi}_i^{(p)}}{\overset{+}{\xi}_i^{(q)}} \quad \text{and} \quad \overset{-}{\rho}_i^{(pq)} = \frac{\overset{-}{\xi}_i^{(p)}}{\overset{-}{\xi}_i^{(q)}}. \tag{16}$$

To each element in $\overset{+}{\boldsymbol{\rho}}^{(pq)}$ and $\overset{-}{\boldsymbol{\rho}}^{(pq)}$, we assign coordinates $\overset{+}{\phi}_i = \frac{\sum_{k=1}^{i} \overset{+}{\xi}_k^{(q)} - \overset{+}{\xi}_i^{(q)}/2}{\sum_{k=1}^{N_{ext}} \overset{+}{\xi}_k^{(q)}}$ and $\overset{-}{\phi}_i = \frac{\sum_{k=1}^{i} \overset{-}{\xi}_k^{(q)} - \overset{-}{\xi}_i^{(q)}/2}{\sum_{k=1}^{N_{ext}} \overset{-}{\xi}_k^{(q)}}$. Finally, we define the continuous functions $\overset{+}{h}(\overset{-}{\phi})$ and $\overset{-}{h}(\overset{-}{\phi})$ that interpolate

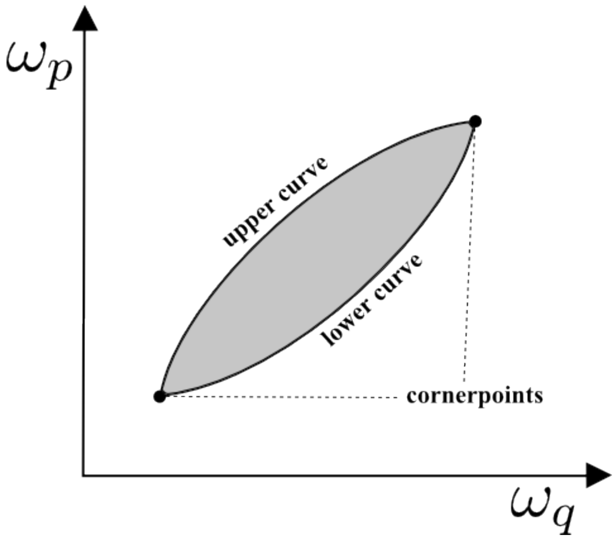

Figure 5: Example of a 'shuttle'-shaped uncertainty region.

the points $\left(\overset{+}{\rho}_i^{(pq)}, \overset{+}{\phi}_i\right)$ and $\left(\overset{-}{\rho}_i^{(pq)}, \overset{-}{\phi}_i\right)$. The lower and upper curve are then described by equation 17.

$$\begin{aligned} \text{lower curve : } \quad & \overset{+}{c}\,(\overset{+}{\phi}) :\rightarrow \begin{cases} \omega_p(t) = \int_{\overset{+}{\phi}=0}^{t} \overset{+}{h}\,(\overset{+}{\phi}) d\,\overset{+}{\phi} \\ \omega_q(t) = \int_{\overset{+}{\phi}=0}^{t} d\,\overset{+}{\phi} \end{cases} \\ \text{upper curve : } \quad & \overset{-}{c}\,(\overset{-}{\phi}) :\rightarrow \begin{cases} \omega_p(t) = \int_{\overset{-}{\phi}=0}^{t} \overset{-}{h}\,(\overset{-}{\phi}) d\,\overset{-}{\phi} \\ \omega_q(t) = \int_{\overset{-}{\phi}=0}^{t} d\,\overset{-}{\phi} \end{cases} \end{aligned} \tag{17}$$

Figure 6 illustrates the process described above.

4.4 Observations

In the 2D-projections of the uncertain region we can clearly see the effect of a varying Young's modulus. We examine 7 cases of increasing maximum gradient. The extreme values of the Young's modulus are 210 GPa and $1.2 \cdot 210 = 252$ GPa. From figures 7 to 10, that show some 2D projections for all 7 cases, a few observations can be made:

1. Increasing the maximum gradient does not change the cornerpoints, as these depend on the extreme values of the Young's modulus itself, but the uncertain region does change. The shuttle-shaped regions become wider, effectively decreasing the dependency between the frequencies as the gradient increases.

2. For lower frequencies, the effect of increasing the gradient on the uncertain region appears to saturate. This saturation effect is much less outspoken for higher frequencies.

3. Some frequencies, such as 5 and 8 (figure 9), appear to be much more interdependent than others, which can be seen from the relatively slim shuttle shape. The increased maximum gradient appears to have little effect on the dependency between these frequencies.

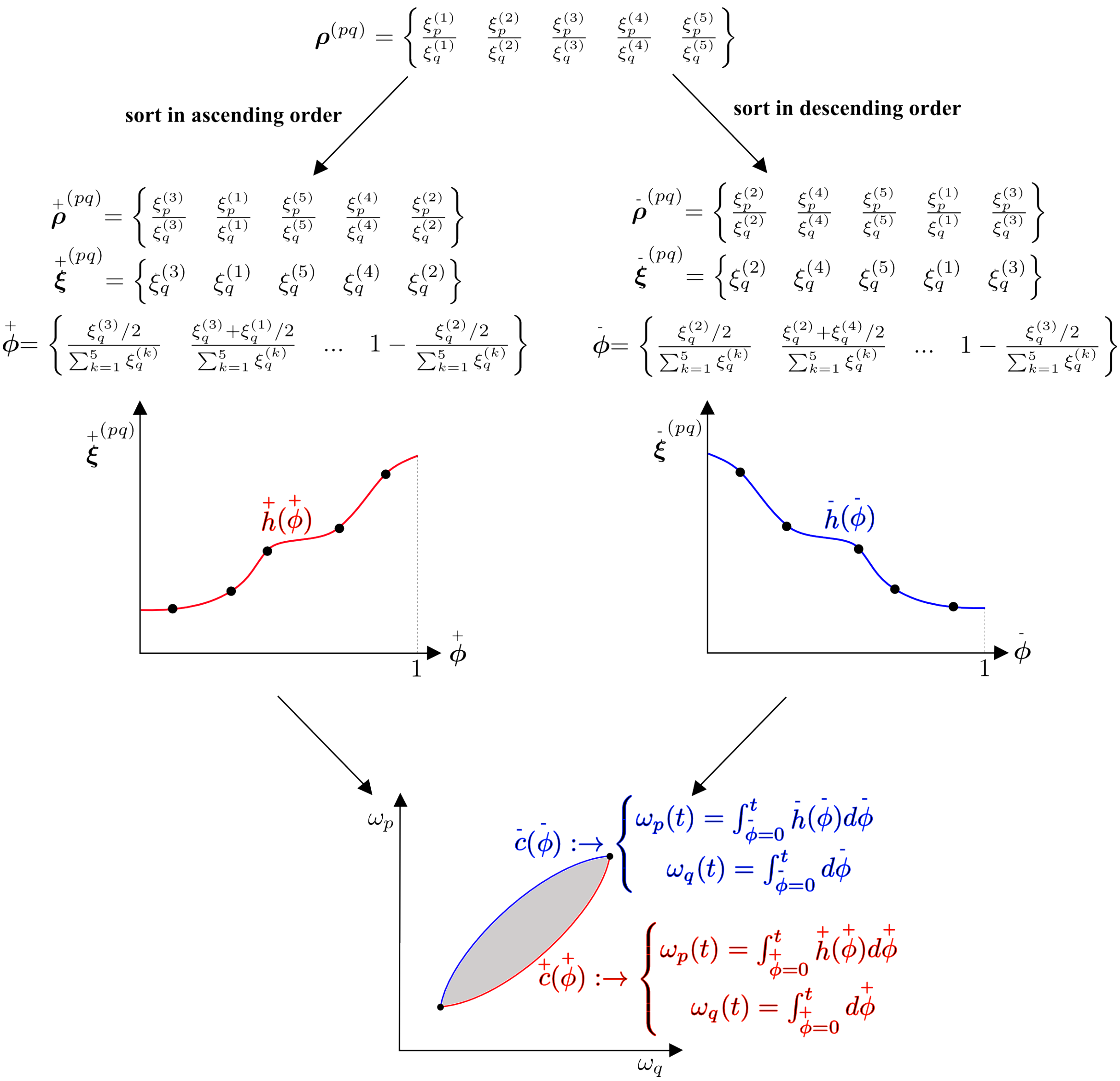

Figure 6: illustration of the process to determine the uncertain region, for the case of only 5 fields $\boldsymbol{\xi}^{(i)}$.

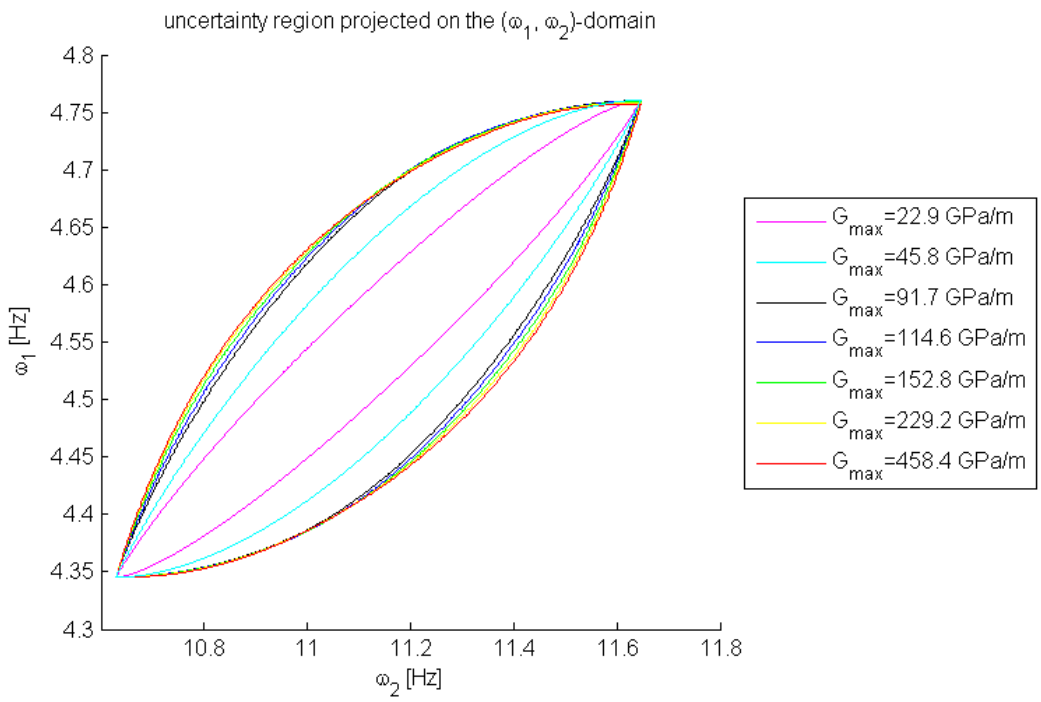

Figure 7: uncertainty region projected on the (ω_1, ω_2)-plane.

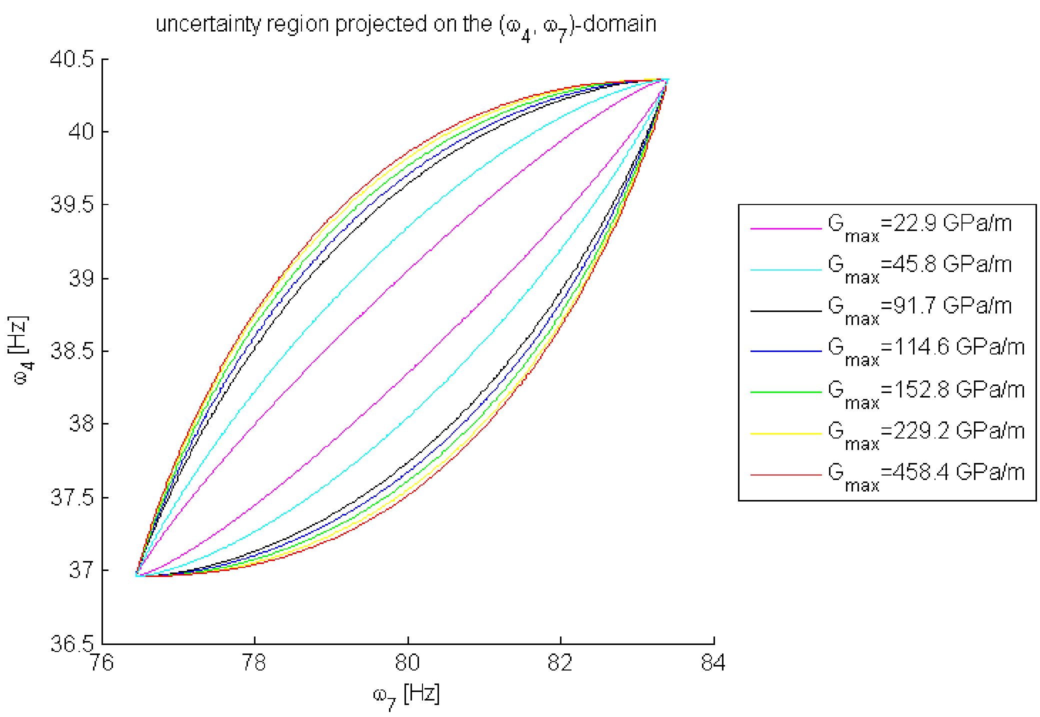

Figure 8: uncertainty region projected on the (ω_4, ω_7)-plane.

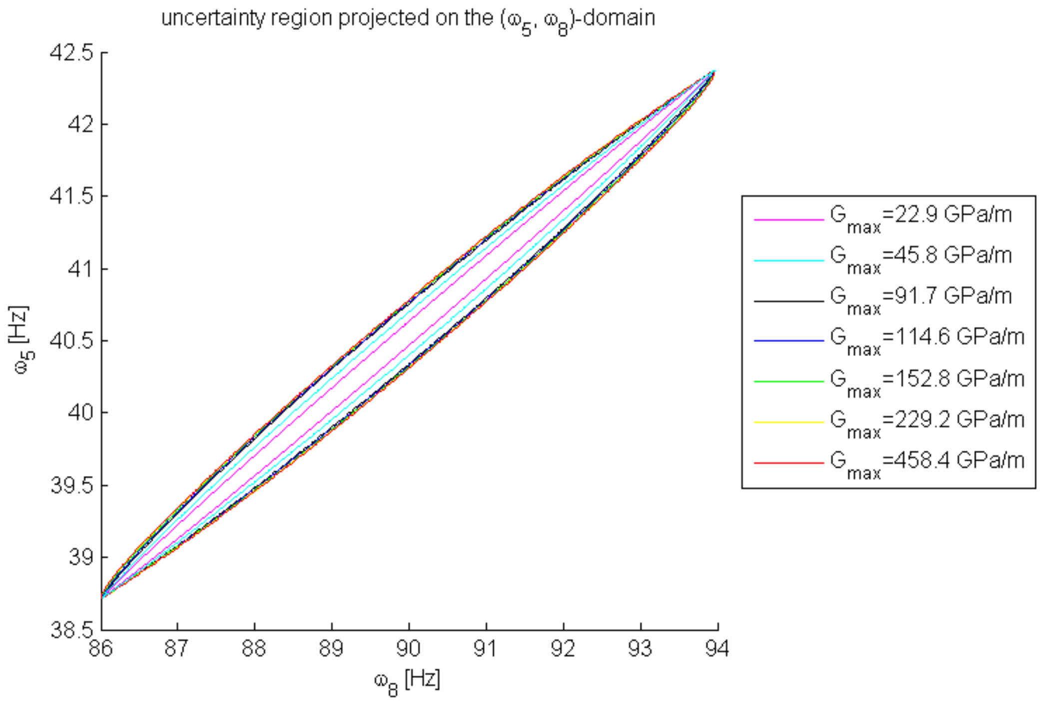

Figure 9: uncertainty region projected on the (ω_5, ω_8)-plane.

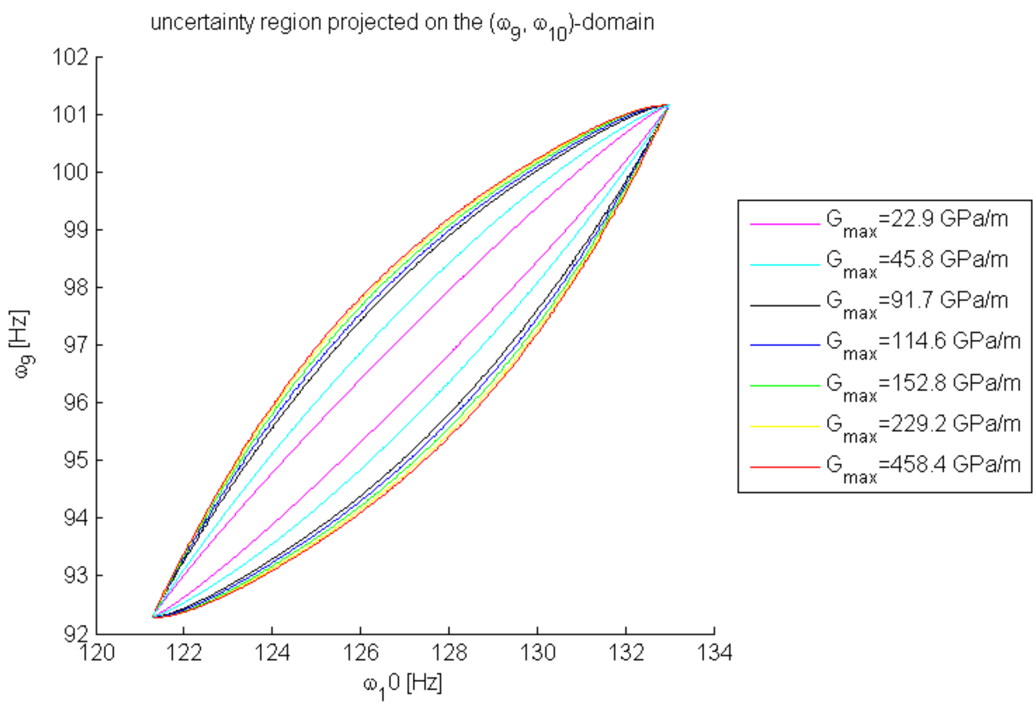

Figure 10: uncertainty region projected on the (ω_9, ω_{10})-plane.

5 CONCLUDING REMARKS & FUTURE RESEARCH TOPICS

In a possiblistic framework, the inability to use correlation forces us to look at dependency at a more general level. According to the authors, the shape of the uncertain region itself holds the most information not only on the degree of dependency between parameters, but also on the nature of it. In this paper, the interval concept is specifically designed towards the fast computation of these regions. For the purpose of monotonous and linear behaviours, which lead to so-called 'shuttle'-shaped uncertain regions, this paper introduced an easy way of computing them without the need of additional simulations. Further research will be done towards formulating relationships between interval field formulations and uncertain region shapes, for non-linear and also non-monotonous input-output relations.

REFERENCES

[1] D. Moens, M. De Munck, W. Desmet, D. Vandepitte, Numerical dynamic analysis of uncertain mechanical structures based on interval fields, IUTAM 2009, *IUTAM Symposium on the Vibration Analysis of Structures with Uncertainties* VOL. 27(2011) 71-83.

[2] W. Verhaeghe, W. Desmet, D. Vandepitte, D. Moens, Interval fields to represent uncertainty on the output side of a static Finite Element analysis, *Computational Methods in Applied Mechanical Engineering* 260(2013) 50-63.

[3] E.Vanmarcke, Random Fields: analysis and synthesis, MIT Press, Cambridge, 1993.

[4] M. Imholz, D. Vandepitte, D. Moens, Derivation of an input interval field decomposition based on expert knowledge using locally defined basis functions, UNCECOMP 2015, *proceedings of UNCECOMP 2015*, Hersonissos, Greece.

[5] M. Imholz, D. Vandepitte, D. Moens, Application of interval fields to geometric output quantities of Finite Element models, UNCERTAINTIES 2016, *proceedings of UNCERTAINTIES 2016*, Maresias, Brazil .